

α_{1B} N-Type Calcium Channel Isoforms with Distinct Biophysical Properties

ANTHONY STEA,^a STEFAN J. DUBEL,^b AND TERRY P. SNUTCH^{b,c}

^aUniversity-College of the Fraser Valley, 33844 King Road, Abbotsford, B.C., Canada V2S 7M8

^bBiotechnology Laboratory, Room 237-6174 University Boulevard, University of British Columbia, Vancouver, B.C. Canada V6T 1Z3

ABSTRACT: N-type calcium channels both generate the initial calcium signal to trigger neurotransmitter release and also interact with synaptic release proteins at many mammalian central nervous system synapses. Two isoforms of the α_{1B} N-type channel from rat brain (α_{1B-I} and α_{1B-II}) were found to differ in four regions: (1) a glutamate (Glu) to glycine (Gly) substitution in domain I S3; (2) a Gly to Glu substitution in the domain I-II linker; (3) the insertion or deletion of an alanine (Ala) in the domain I-II linker; and (4) the presence or absence of serine/phenylalanine/methionine/glycine (SFMG) in the linker between domain III S3-S4. Comparison of the electrophysiological properties of the α_{1B-I} and α_{1B-II} N-type channels shows that they exhibit distinct kinetics as well as altered current-voltage relations. Utilizing chimeric α_{1B-I} and α_{1B-II} cDNAs, we show that: (1) the Glu 177 to Gly substitution in domain I S3 increases the rate of activation by ~15-fold; (2) the presence or absence of Ala 415 in the domain I-II linker alters current-voltage relations by ~10 mV but does not affect channel kinetics; (3) the substitution of Gly 387 to Glu in the domain I-II linker also has no effect on kinetics; and (4) the presence or absence of SFMG (1236-1239) in domain III S3-S4 did not significantly affect channel current-voltage relations, kinetics, or steady state inactivation. We conclude that molecularly distinct α_{1B} isoforms are expressed in rat brain and may account for some of the functional diversity of N-type currents in native cells.

Voltage-gated calcium channels contribute to a number of physiological processes in the nervous system, including the regulation of calcium-dependent enzymes and gene transcription, the shaping of action potentials and firing patterns, and the initiation of neurotransmitter release. Of the four major classes of native neuronal calcium channels described to date (L-, N-, P/Q-, and T-types), N-type and P/Q-type channels are localized to presynaptic terminals and contribute to neurotransmitter release.¹⁻⁵ While both N-type and P/Q-type channels are inhibited by the neuropeptide toxin ω -conotoxin MVIIC (ω -CTX-MVIIC), N-type channels can be pharmacologically isolated by their selective and irreversible block by ω -conotoxin GVIA (ω -CTX-GVIA).⁶⁻⁸ In contrast, P/Q-type channels are preferentially blocked by the spider toxin, ω -agatoxin IVA (ω -AGA-IVA).⁹ Examination of central and peripheral neurons has revealed native N-type currents with distinct single-channel, kinetic, and voltage-dependent properties.¹⁰⁻¹⁴ While a number of kinetic models have been proposed to account for the heterogeneous gating characteristics of N-type channels,^{11,15-17} the exact molecular determinants involved remain to be precisely defined.

^cCorresponding author: Dr. Terry P. Snutch, Biotechnology Laboratory, Rm. 237-6174 University Blvd., University of British Columbia, Vancouver, B.C. Canada V6T 1Z3. Phone: 604-822-6968; fax: 604-822-6470; e-mail: snutch@zoology.ubc.ca

High-threshold neuronal calcium channels (L-, N-, P/Q-types) are heterotrimeric complexes consisting of a pore-forming α_1 subunit containing four conserved structural domains, a β subunit that interacts cytoplasmically with the α_1 subunit domain I-II linker, and an $\alpha_2\delta$ subunit that contains a single transmembrane segment covalently linked to an extracellular component (reviewed in Ref. 18). Molecular cloning and expression studies have documented a larger degree of calcium channel diversity than predicted from pharmacological and electrophysiological studies. To date, four different α_1 subunit genes encoding L-type channels and two genes encoding T-type channels have been described. N-type, P/Q-type, and a novel type (α_{1E}) are each encoded by single genes¹⁸⁻²¹ (see TABLE 1). With the exception of the T-type α_{1G} and α_{1H} subunits, the kinetic and current-voltage-dependent properties of currents induced by the α_1 subunits is modulated by coexpression any one of four different β subunits ($\beta 1$ - $\beta 4$).²²⁻²⁴

TABLE 1. Pharmacological Profiles of Cloned and Native Calcium Currents

α_1 Subunit Gene	ω -CTX- GVIA	Dihydropyridines	ω -AGA-IVA	ω -CTX- MVIIC	Native Channel Type
α_{1A}	-	-	✓	✓	P/Q-type
α_{1B}	✓	-	-	✓	N-type
α_{1C}	-	✓	-	-	L-type
α_{1D}	-	✓	-	-	L-type
α_{1E}	-	-	-	-	Novel
α_{1F}	?	?	?	?	L-type ^a
α_{1G}	-	-	-	-	T-type
α_{1H}	-	-	-	-	T-type
α_{1S}	-	✓	-	-	L-type

^a α_{1F} is predicted to be an L-type channel based on the conservation of residues that confer dihydropyridine sensitivity.²¹

Within most classes of α_1 subunits, closely related isoforms have been identified (reviewed in Ref. 18), although there are only a few conclusive reports demonstrating alternative splicing as the mechanism for generating calcium channel diversity.²⁵⁻²⁷ We have previously reported the cloning and expression of α_{1B} N-type channel isoforms derived from rat brain,²⁸⁻³¹ and Lipscombe and coworkers³² have recently reported further α_{1B} isoforms expressed in rat sympathetic ganglia. Together with a number of α_{1B} variants found in mouse, rabbit, and humans,³³⁻³⁵ it is apparent that multiple α_{1B} N-type isoforms are expressed both across species and between tissues and cell types within a species. In the present study, we report that the rat brain α_{1B-I} and α_{1B-II} isoforms exhibit distinct biophysical properties which can be attributed to small amino acid alterations in defined regions of the N-type channel α_{1B} subunit.

MATERIAL AND METHODS

Expression of N-type Calcium Channels in Xenopus Oocytes

cDNAs encoding the rat brain calcium channel α_1 subunits, rbB-I (α_{1B-I} ^{28,29}) and rbB-II (α_{1B-II} ^{30,31}) were expressed in *Xenopus* oocytes as described previously.³¹ Briefly, ovaries were surgically removed from anesthetized (0.17% 3-aminobenzoic acid ethyl ester; MS-222) mature female *Xenopus laevis* (*Xenopus* One, Ann Arbor, MI) and agitated for 2–3 h in 2 mg/ml collagenase (type IA; Sigma) dissolved in a Ca-free OR-2 solution containing (mM): NaCl, 82.5; KCl, 2; MgCl₂, 1; HEPES, 5 at a pH of 7.5. Prior to injection, oocytes were allowed to recover for 3–20 h at 18°C in standard oocyte saline (SOS) containing (mM): NaCl, 100; KCl, 2; CaCl₂, 1.8; MgCl₂, 1; HEPES, 5 at a pH of 7.5; supplemented with 2.5 mM sodium pyruvate and 10 μ g/ml gentamycin sulphate (Sigma) or 100 U/ml penicillin-streptomycin. Nuclear injections were performed on stage V and VI oocytes using a Drummond Nanoject Automatic injector. Approximately 1–2 ng of each expression plasmid were injected into the nucleus (~10 nl total volume), and oocytes were maintained in supplemented SOS at 18°C for 2–5 days prior to electrophysiological recording. For this study, three full-length chimeric α_{1B-I} - α_{1B-II} cDNAs (α_{1B-7} , α_{1B-39} , α_{1B-52}) were constructed into the vertebrate expression vector, pMT2³⁶ (see TABLE 2). Some experiments were also performed on another construct (30-14G) that is identical to α_{1B-II} except that it contains Gly 387 rather than Glu 387 (see Refs. 37,38). In all experiments the α_{1B} cDNAs were always coexpressed with the β_{1B} subunit.

Solutions and Data Analysis

Two-microelectrode voltage clamp experiments were performed on *Xenopus* oocytes using Axoclamp-2A or Geneclamp 500 amplifiers (Axon Instruments, Burlingame, CA) connected to an IBM-compatible computer with PCLAMP software (Axon Instruments). Microelectrodes were filled with 3 M KCl and typically had resistances of 0.5 to 1.5 M Ω . Ba currents were isolated by recording in a solution containing (mM): BaCl₂, 40; KCl, 2; tetraethylammonium chloride, 36; 4-amino-pyridine, 5; niflumic acid, 0.4; 5-nitro-2-(3-phenylpropylamino) benzoic acid (NPPB), 0.2; HEPES, 5 at pH 7.6. Many oocytes were injected with 10–30 nl of 100 mM BAPTA-free acid (10 mM HEPES, pH 7.2 with CsOH) to chelate intracellular calcium and prevent Ca-activated chloride current contamination.

Current recordings were capacitance and leak subtracted and filtered at 1000 Hz. Voltage-dependent properties were determined by fitting normalized current-voltage relations and steady-state inactivation data with smooth Boltzmann curves. Activation and inactivation rates were determined by fitting with single exponential curves. Oocytes expressing less than 100 nA of peak Ba current were not used in this study. Only cells with little or no endogenous chloride current (as indicated by an absence of chloride tail currents) were used in the analysis of current kinetics. Significant differences between various parameters were determined using a Student's *t*-test with the significance level set at $p \leq 0.01$. All values given in the text and figures are mean \pm standard error of the mean.

RESULTS

The initial characterization of a full-length rat brain N-type channel α_1 subunit (called rbB-I or α_{1B-I}) revealed slowly activating and inactivating whole-cell currents that were irreversibly blocked by 1–2 μM ω -CTX-GVIA (FIG. 1B and Refs. 28,29). The subsequent isolation of a second full-length α_{1B} cDNA (called rbB-II or α_{1B-II}) revealed a fast-activating and -inactivating ω -CTX-GVIA-sensitive current that was more similar to that of native N-type currents (FIG. 1C and Refs. 30,31). Compared to α_{1B-I} , the rat brain α_{1B-II} N-type channel isoforms differ in four regions: (1) a G to A transition resulting in a glutamate (Glu) to glycine (Gly) substitution at aa # 177 in domain I S3; (2) an A to G transition resulting in a Gly to Glu substitution at aa # 387 in the domain I-II linker; (3) the deletion of three base pairs (bp) in the domain I-II linker resulting in the absence of an alanine (Ala) at aa # 415; and (4) the deletion of 12 bp in the domain III S3-S4 loop resulting in the absence of four amino acids—serine, phenylalanine, methionine, glycine (SFMG) at aa # 1236–1239 (FIG. 1A).

In addition to the rat brain α_{1B-I} and α_{1B-II} isoforms, a number of α_{1B} variants have also been described in rat sympathetic ganglia³² as well as in mouse, rabbit, and human.^{33–35} To date, only the rat brain α_{1B-I} (rbB-I) isoform exhibits Glu 177 in domain I S3, while the rat brain α_{1B-II} and all other N-type channels possess Gly at this position. In contrast, only the rat brain α_{1B-II} isoform exhibits a Glu residue at position 387 in the domain I-II linker, while α_{1B-I} and all other N-type channels possess a Gly at this position. The presence or absence of Ala 415 in the domain I-II linker appears to be a prevalent N-type channel variant and has now been found in rat and mouse brain as well as in rat sympathetic ganglia. To date, the presence of the tetrapeptide SFMG in domain III S3-S4 has been detected in α_{1B} transcripts from rat brain and sympathetic ganglia and also in mouse brain (Genbank accession #2811218). Although not found in either of the rat brain α_{1B-I} or α_{1B-II} subtypes, rat sympathetic ganglia and mouse and human neuroblastomas express additional variants exhibiting the presence or absence of the dipeptide Glu/Thr in the domain IV S3-S4 linker.^{32–35}

Comparison of the whole cell properties of α_{1B-I} and α_{1B-II} N-type channels shows that they exhibit striking differences in their kinetic properties (FIG. 1B and 1C). The α_{1B-II} currents exhibit fast activation ($\tau_{\text{act}} = 2.8 \pm 0.2$ ms) and inactivation ($\tau_{\text{inact}} = 112.1 \pm 9.7$ ms) compared to the slowly activating ($\tau_{\text{act}} = 41 \pm 3.6$ ms) and inactivating ($\tau_{\text{inact}} = 576.5 \pm 97.9$ ms) α_{1B-I} whole-cell currents (also see TABLE 2). This is more clearly observed with a 2 s depolarizing step (FIG. 2A).

In addition to the kinetic differences, a significant affect on current-voltage relation is also observed, with the α_{1B-II} current-voltage relation being shifted ~ 10 mV to the right of the α_{1B-I} (FIG. 2B and TABLE 2). There was no significant difference between the steady state inactivation curves of the two N-type channel isoforms (FIG. 2C and TABLE 1). Both α_{1B-I} and α_{1B-II} currents showed a range of expression of peak Ba currents from 100 nA to well over 2 μA ($\alpha_{1B-I} = 817 \pm 312$ nA, $n = 9$; $\alpha_{1B-II} = 1210 \pm 182$ nA, $n = 32$). The size of whole-cell currents did not significantly affect channel kinetics.

In order to determine the amino acid residues responsible for the kinetic and voltage-dependent differences between α_{1B-I} and α_{1B-II} N-type channels, several chimeric cDNAs were constructed and subsequently expressed in *Xenopus* oocytes. TABLE 2 summarizes the differences in the amino acid composition of the three chimeras (α_{1B-7} , α_{1B-39} , and α_{1B-52}) in the four specific regions of variation between α_{1B-I} and α_{1B-II} . The chimera α_{1B-39} ,

TABLE 2. Summary of the Electrophysiological Characteristics of Rat Brain α_{1B} Channels

α_{1B} cDNA	τ act ^a (ms)	τ inact ^b (ms)	V_{50} act ^c (mV)	V_{50} inact ^d (mV)
α_{1B-I} ^e (E, G, +A, +SFMG)	41.0 ± 3.6 (n = 9)	576.5 ± 97.9 (n = 6)	-0.1 ± 1.9 (n = 7)	-63.5 ± 1.68 (n = 6)
α_{1B-II} ^f (G, E, -A, -SFMG)	2.8 ± 0.2* (n = 15)	112.1 ± 9.7* (n = 15)	+9.7 ± 0.8* (n = 21)	-67.5 ± 2.9 (n = 5)
α_{1B-7} (G, E, -A, +SFMG)	2.9 ± 0.2* (n = 20)	128.5 ± 8.5* (n = 17)	+9.4 ± 1.6* (n = 17)	-67.1 ± 1.2 (n = 14)
α_{1B-52} (E, G, -A, +SFMG)	37.8 ± 3.1 (n = 15)	633.4 ± 64.1 (n = 9)	+19.4 ± 1.0* (n = 10)	-57.5 ± 1.3 (n = 7)
α_{1B-39} (E, G, +A, -SFMG)	57.5 ± 14.3 (n = 4)	726.0 ± 88.6 (n = 3)	+4.6 ± 0.7 (n = 3)	-57.7 ± 2.8 (n = 3)

^aSingle exponential curves were fitted to the initial activation phase of the inward Ba currents and τ values (ms) given in text.

^bSingle exponential curves were fitted to the decaying inactivation phase of the inward Ba currents and τ values (ms) given in text.

^cThe half-point of activation of the current-voltage relation was calculated by smooth curves fit to the raw I/V data.

^dThe half-point of the steady state inactivation curve was calculated by a smooth Boltzmann curve fit to data calculated from peak currents elicited from various holding potentials for 20 s.

^eFor a detailed survey of α_{1B-I} electrophysiology and pharmacology see Ref. 29.

^fFor a detailed survey of α_{1B-II} electrophysiology and pharmacology see Ref. 31.

* $p \leq 0.01$, Student's *t*-test, compared to α_{1B-I} as control.

which is identical to α_{1B-I} except that it is missing the SFMG in the putative extracellular loop between S3 and S4 of domain III, exhibited similar kinetics and current-voltage properties as α_{1B-I} (FIG. 3 and TABLE 2). Furthermore, the deletion of SFMG in α_{1B-II} did not affect sensitivity to ω -CTX-GVIA (FIG. 1; $n = 11$).

The presence or absence of Ala 415 in the domain I-II linker did not appear to be a determining factor of N-type channel kinetics since the α_{1B-52} channel differs from α_{1B-I} only by the Ala 415 deletion and has similar slow kinetics (FIG. 4A, TABLE 2). However, the current-voltage relation for the α_{1B-52} clone was significantly shifted ~19 mV to the right of the α_{1B-I} (FIG. 4B, TABLE 2). This rightward shift is similar to that seen for α_{1B-II} (TABLE 2), although even greater in magnitude. The steady state inactivation of α_{1B-52} was not significantly different than that of α_{1B-I} ($V_{50inact} = -58, -64$, respectively; FIG. 4C, TABLE 2).

The other two differences in α_{1B-II} compared to α_{1B-I} are amino acid substitutions with Gly at position 177 instead of Glu 177 in domain I S3, and Glu 387 instead of Gly 387 in the domain I-II cytoplasmic linker region. Gly 387 is highly conserved among cloned calcium channels.¹⁸ Electrophysiological analyses of a full-length α_{1B-II} construct containing

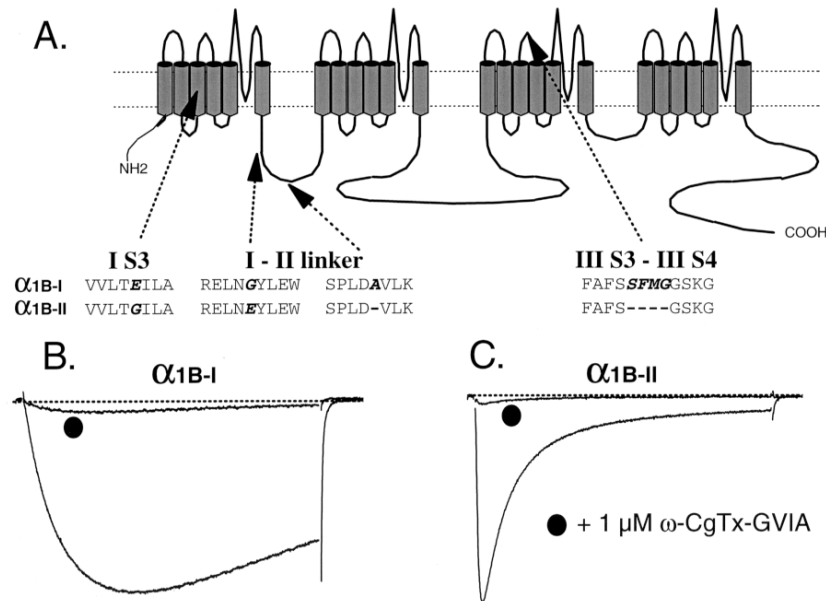


FIGURE 1. Amino acid sequence and functional differences between rat brain α_{1B-I} and α_{1B-II} N-type calcium channels. **A.** Schematic representation of sequence differences between α_{1B-I} and α_{1B-II} . **B.** α_{1B-I} peak current traces in the presence and absence of 1 μ M ω -CTX-GVIA (400 ms step from -100 mV to $+20$ mV). Note the slow kinetics of activation and inactivation. **C.** α_{1B-II} peak current traces in the presence and absence of 1 μ M ω -CTX-GVIA (400 ms step from -100 mV to $+20$ mV).

Gly 387 (called 30-14G) showed fast kinetics ($n = 5$, not shown; and also see Refs. 37,38) indicating that Glu 387 is not a determining factor for channel kinetics. The most likely candidate for speeding the activation and inactivation kinetics of α_{1B-II} compared to α_{1B-I} is the Glu 177 to Gly 177 substitution in domain I S3. This is clearly seen in Figure 5 between constructs including the Gly 177, which display fast activation (α_{1B-II} , α_{1B-7}) and constructs with the Glu 177 in domain I S3, which show slowed kinetics (α_{1B-I} , α_{1B-52} , α_{1B-39} ; TABLE 2). N-type channel inactivation kinetics were similarly affected by the Glu 177 to Gly 177 substitution (FIG. 5B and TABLE 2).

DISCUSSION

Species-specific α_{1B} N-type channel isoforms have been cloned from mouse, rabbit, human, and rat.²⁸⁻³⁵ Furthermore, native N-type currents from a variety of cell types and preparations exhibit distinct gating properties.¹⁰⁻¹⁴ Attempts to correlate cloned α_1 subunits with native Ca currents are complicated by the fact that it is difficult to determine whether cross-species DNA sequence differences represent evolutionary divergence or

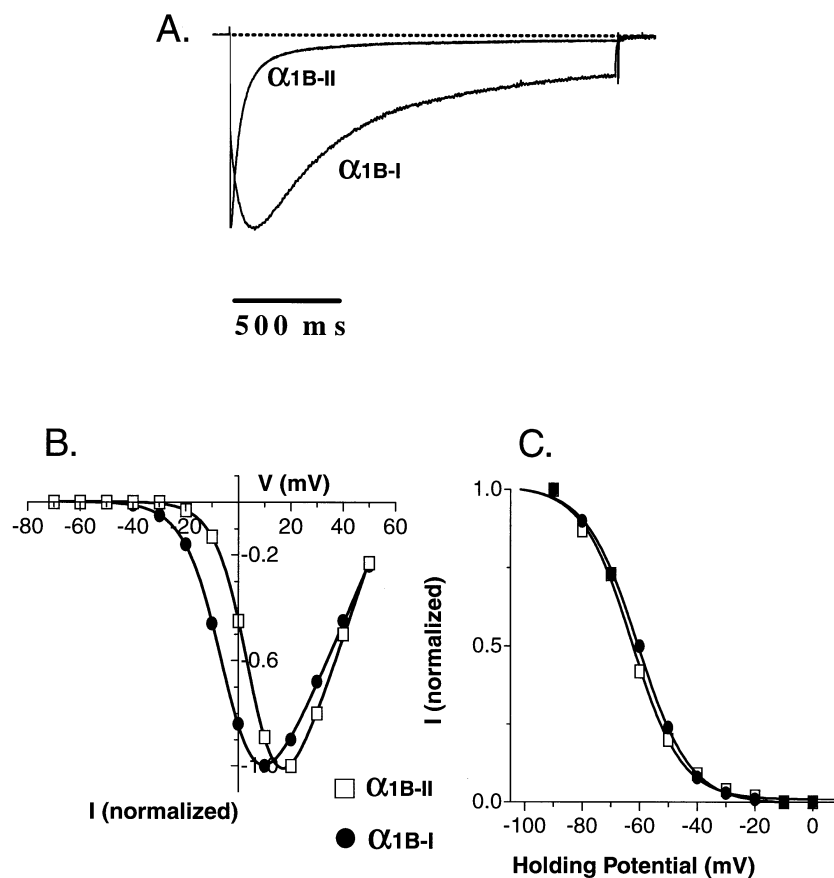


FIGURE 2. Kinetics and voltage-dependent differences between α_{1B-I} and α_{1B-II} N-type currents. **A.** Long test pulses (2 s steps from 100 mV to +20 mV) show increased activation and inactivation rates of the α_{1B-II} isoform. **B.** Current-voltage relation shows an ~ 10 mV depolarized shift in α_{1B-I} . **C.** Steady state inactivation curves are not significantly different between α_{1B-I} and α_{1B-II} .

rather than alternatively spliced variants are differentially expressed spatially and temporally. In the present paper we show that two rat brain α_{1B} N-type channel isoforms, α_{1B-I} and α_{1B-II} (or rbB-I and rbB-II), exhibit distinct electrophysiological properties. Together with the recent report of Lin and coworkers³² describing α_{1B} isoforms expressed in rat sympathetic ganglia, the results suggest that multiple functionally distinct α_{1B} N-type calcium channels are expressed in mammalian neurons.

Examination of chimeric cDNAs constructed between different α_1 subunit genes together with *in vitro* mutagenesis studies have identified regions important for permeation, activation, excitation-contraction coupling, and β subunit binding.³⁹⁻⁴² In the

present study, we examine chimeric channels derived from isoforms within a single class of α_1 subunit gene and find that modest amino acid alterations can have dramatic effects on N-type calcium channel functional properties. Of the four regions of amino acid difference between α_{1B-I} and α_{1B-II} , two were found to significantly alter whole-cell N-type current characteristics. First, the single amino acid substitution of Glu 177 to Gly 177 in domain I S3 dramatically affected N-type channel activation and inactivation kinetics. Compared to the kinetically slower α_{1B-I} containing Glu 177, the α_{1B-II} subunit with Gly at this site exhibited an approximately 15-fold faster activation rate and an approximately 5-fold faster inactivation rate. The effect of substitutions in domain I S3 of N-type channel

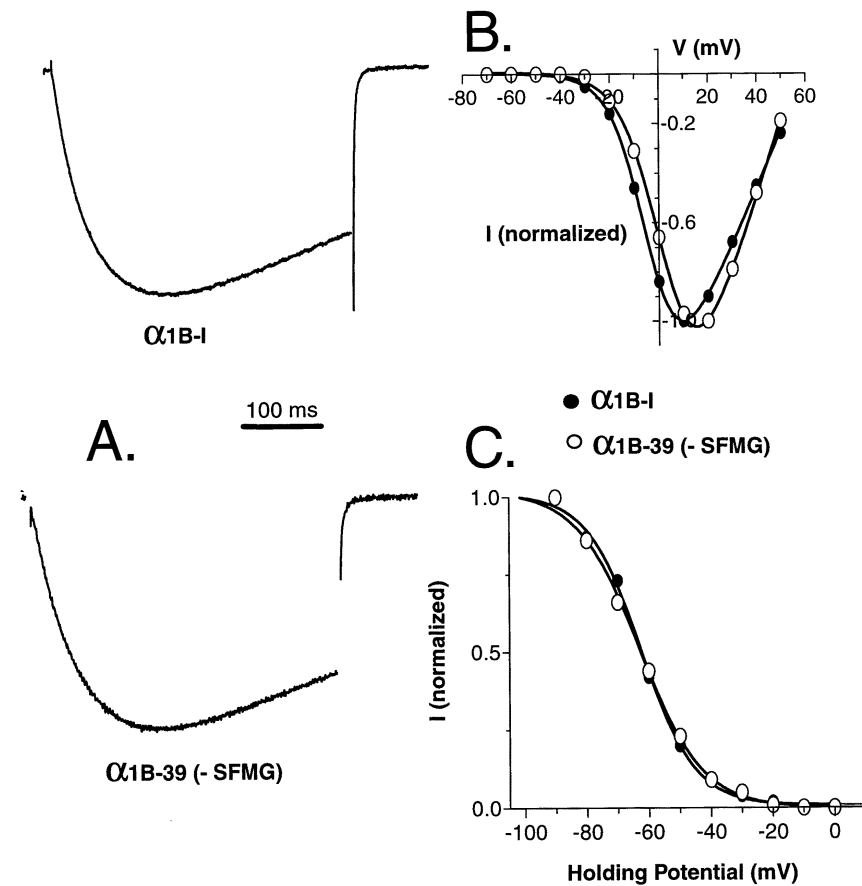


FIGURE 3. Deletion of the tetrapeptide SFMG in the extracellular loop between domain III S3 and III S4 does not alter kinetics or voltage dependence of α_{1B} N-type channels. **A.** Peak current traces of α_{1B-I} and α_{1B-39} show similar kinetics. **B.** Current-voltage relations of α_{1B-I} and α_{1B-39} show no significant differences. **C.** Steady state inactivation properties of α_{1B-I} and α_{1B-39} are similar to each other.

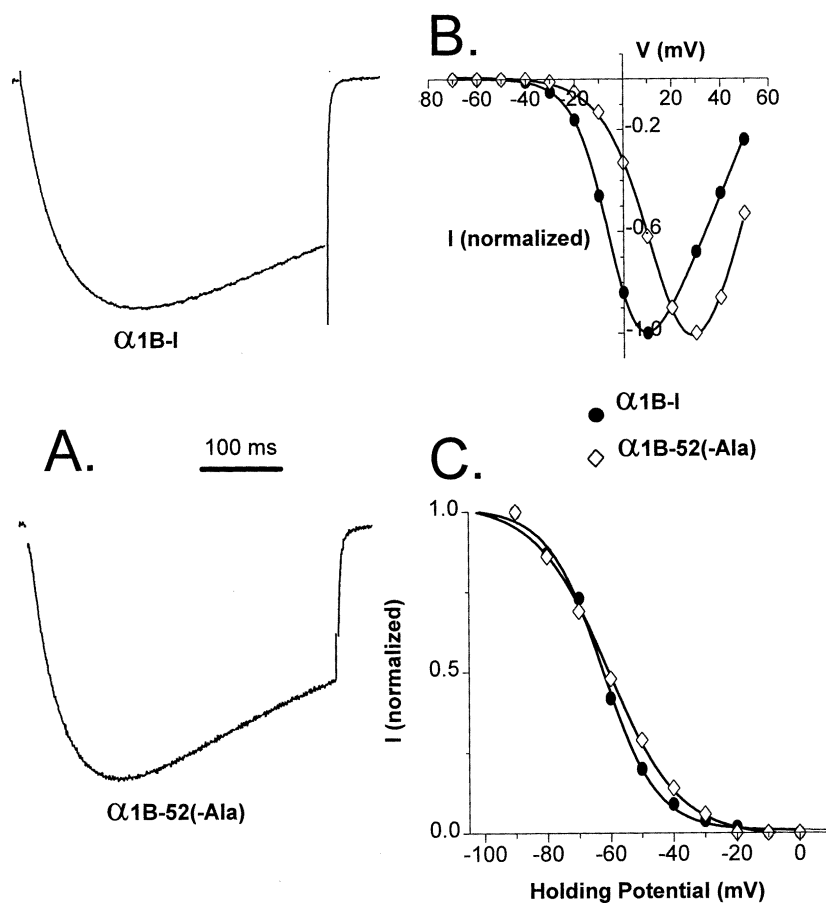


FIGURE 4. Deletion of a single alanine (Ala) residue in the domain I-II intracellular loop alters voltage dependence but not kinetics of α_{1B} currents. **A.** Peak current traces of α_{1B-I} and α_{1B-52} show similar kinetics. **B.** Current-voltage relations of α_{1B-52} are shifted 15–20 mV more depolarized compared to α_{1B-I} . **C.** Steady state inactivation curves of α_{1B-I} and α_{1B-52} are not significantly different.

activation kinetics is in agreement with the work of Nakai, Beam, and coworkers examining L-type channel kinetics.⁴¹

In 11 RT-PCR products examined, Lin and coworkers³² did not detect the brain Glu 177 variant in superior cervical ganglia (SCG) neurons. The authors suggest that the dramatically slowed activation kinetics observed between the rat brain α_{1B-I} and other N-type currents is less likely due to the Glu 177 in α_{1B-I} and more likely due to differences in expression levels, which might alter channel properties possibly through G-protein or calcium channel β subunit interactions. In the present study, the levels of rat brain α_{1B-I} and α_{1B-II} -induced whole-cell currents were both similar to each other and to those reported by Lin *et al.*,³² and current size did not affect the kinetics. Indeed, all constructs with the Gly

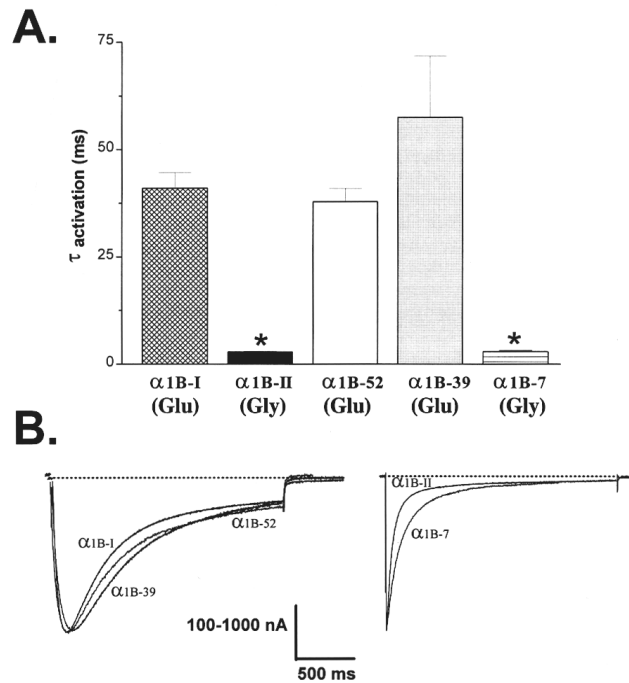


FIGURE 5. Substitution of a glutamate (E) to a glycine (G) in the domain I S3 region alter the kinetics of α_{1B} N-type calcium channels. **A.** The bar chart summarizes the activation rate of various α_{1B} constructs (see TABLE 2) showing the presence of either glutamate (E) or glycine (G) in the domain I S3 region at amino acid #177. Note the fast kinetics of constructs with glycine present. **B.** Long peak current traces (2 s) of the major constructs used in this study, grouping them with either glutamate (*left*; α_{1B-I} , α_{1B-52} , α_{1B-39}) or glycine (*right*; α_{1B-II} and α_{1B-7}) present in the domain I S3 region. The *asterisks* indicate statistical significance (student's *t*-test, $p < 0.01$) as compared to α_{1B-I} .

177 substitution used in this study show that this site in domain I S3 can affect the activation rate by more than an order of magnitude (FIG. 5 and TABLE 2).

The second significant functional difference identified between the α_{1B-I} and α_{1B-II} affects N-type channel current-voltage relations. The presence or absence of Ala 415 in the domain I-II linker resulted in a 10-mV shift in $V_{50\text{act}}$ between the two N-type channel isoforms. Lin and coworkers³² also found that the similar presence or absence of Ala 415 occurs in superior cervical ganglia neurons. In contrast to our results, the authors suggest that the Ala 415 variation has little influence on N-type channel gating, although they did not test this directly with constructs comparing the presence or absence of Ala 415.

Our results suggest that the absence of Ala 415 results in a depolarizing shift in N-type channel current-voltage relations and also that other structural elements are likely to affect current-voltage relations. For example, a comparison of the variants in SCG neurons showed that the presence or absence of SFMG in domain III S3-S4 and the presence or

absence of the dipeptide Glu/Thr in domain IV S3-S4 also shifted N-type current-voltage relations.³² In our study, the insertion or deletion of SFMG did not measurably affect any physiological property of N-type channels. These results underscore the importance of testing all possible chimeric combinations in order to help define sites that might functionally couple to each other.

It should also be noted that both Gly/Glu 387 and Ala 415 are within the β subunit binding site in the domain I-II linker.⁴² Since coexpression of β subunits affects several calcium channel properties, including current-voltage relations and kinetics,²²⁻²⁴ it is possible that alterations in this region could alter α_1 subunit- β subunit interactions, resulting in altered gating.

In order to confirm that the sequence differences between the rat brain α_{1B-I} and α_{1B-II} isoforms reflect alternative splicing of the single α_{1B} gene, it will be necessary to examine rat genomic DNA and intron/exon boundaries. However, genomic analyses of α_{1A} (P/Q-type), α_{1C} (L-type), and α_{1D} (L-type) subunit genes indicate that alternative splicing is a common mechanism to generate calcium channel variants.²⁵⁻²⁷ Together with the data of Lin and coworkers³² showing that α_{1B} isoforms are expressed in a tissue-specific manner, it is likely that most of the reported α_{1B} variants represent bona fide N-type channel variants. The exceptions to this may be Glu 177 in domain I S3 and Gly 387 in the domain I-II linker. Neither of these substitutions has been reported elsewhere, and it is possible that either could result from single base transitions (G to A or A to G) due to reverse transcription errors or to RNA editing. The exact nature of these and all other α_{1B} variants must await the examination of mammalian genomic DNA.

ACKNOWLEDGMENTS

We thank Dr. Mary M. Gilbert for helpful comments on the manuscript. The research was supported by a grant from the Medical Research Council (MRC) of Canada (to T.P.S.) and a postdoctoral fellowship from the MRC (to A.S.). T.P.S. is the recipient of an MRC Scientist Award.

REFERENCES

1. TAKAHASHI, T. & A. MOMIYAMA. 1993. Different types of calcium channels mediate central synaptic transmission. *Nature* **366**: 156-158.
2. WHEELER, D.B., A. RANDALL & R.W. TSIEN. 1994. Role of N-type and Q-type Ca channels in supporting hippocampal synaptic transmission. *Science* **264**: 107-111.
3. DUNLAP, K., J.I. LUEBKE & T.J. TURNER. 1995. Exocytotic Ca^{2+} channels in mammalian central neurons. *Trends Neurosci.* **18**: 89-98.
4. WESTENBROEK, R.E., J.W. HELL, C. WARNER, S.J. DUBEL, T.P. SNUTCH & W.A. CATTERALL. 1992. Biochemical properties and subcellular distribution of an N-type calcium channel α_1 subunit. *Neuron* **9**: 1-20.
5. WESTENBROEK, R.E., T. SAKURAI, E.M. ELLIOTT, J.W. HELL, T.V.B. STARR, T.P. SNUTCH & W.A. CATTERALL. 1995. Immunohistochemical identification and subcellular distribution of the α_{1A} subunits of brain calcium channels. *J. Neurosci.* **15**: 6403-6418.
6. OLIVERA, B.M., J.M. MCINTOSH, L.J. CRUZ, F.A. LUQUE & W.R. GRAY. 1984. Purification and sequence of a presynaptic peptide toxin from *Conus geographus* venom. *Biochemistry* **23**: 5087-5090.
7. BOLAND, L.M., J.A. MORRILL & B.P. BEAN. 1994. ω -Conotoxin block of N-type calcium channels in frog and rat sympathetic neurons. *J. Neurosci.* **14**: 5011-5027.

8. HILLYARD, D.R., V.D. MONJE, I.M. MINTZ, B.P. BEAN, L. NADASDI, J. RAMACHANDRAN, G. MILJANICH, A. AZIMI-ZOONOZ, J.M. MCINTOSH, L.J. CRUZ, J.S. IMPERIAL & B.M. OLIVERA. 1992. A new *Conus* peptide ligand for mammalian presynaptic Ca²⁺ channels. *Neuron* **9**: 69–77.
9. MINTZ, I.M., V.J. VENEMA, K.M. SWIDEREK, T.D. LEE, B.P. BEAN & M.E. ADAMS. 1992. P-type channels blocked by the spider toxin ω -Aga-IVA. *Nature* **355**: 827–829.
10. LIPSCOMBE, D., S. KONGSAMUT & R.W. TSJEN. 1989. α -adrenergic inhibition of sympathetic neurotransmitter release mediated by selective modulation of N-type calcium channel gating. *Nature* **340**: 639–642.
11. BEAN, B.P. 1989. Neurotransmitter inhibition of neuronal calcium currents by changes in channel voltage dependence. *Nature* **340**: 153–156.
12. PLUMMER, M.R., D.E. LOGOTHETIS & P. HESS. 1989. Elementary properties and pharmacological sensitivities of calcium channels in mammalian peripheral neurons. *Neuron* **2**: 1453–1463.
13. JONES, S.W. & T.N. MARKS. 1989. Calcium currents in bullfrog sympathetic neurones: II inactivation. *J. Gen. Physiol.* **94**: 169–182.
14. PLUMMER, M.R. & P. HESS. 1991. Reversible uncoupling of inactivation in N-type calcium channels. *Nature* **351**: 657–659.
15. ELSMLIE, K.S., W. ZHOU & S.W. JONES. 1990. LHRH and GTP- γ -S modify calcium currents activation in bullfrog sympathetic neurons. *Neuron* **5**: 75–80.
16. BOLAND, L.M. & B.P. BEAN. 1993. Modulation of N-type calcium channels in bullfrog sympathetic neurons by luteinizing hormone-releasing hormone: Kinetics and voltage-dependence. *J. Neurosci.* **14**: 516–533.
17. PATIL, G., M. DE LEON, R.R. REED, S. DUBEL, T.P. SNUTCH & D.T. YUE. 1996. Elementary events underlying voltage-dependent G-protein inhibition of N-type calcium channels. *Biophys. J.* **71**: 2509–2521.
18. STEPA, A., T.W. SOONG & T.P. SNUTCH. 1995. Voltage-gated calcium channels. *In* Handbook of Receptors and Channels; Ligand- and Voltage-Gated Ion Channels. R. Alan North, Ed.: 113–152. CRC Press. Boca Raton, Florida.
19. PEREZ-REYES E., L.L. CRIBBS, A. DAUD, A.E. LACERDA, J. BARCLAY, M.P. WILLIAMSON, M. FOX, M. REES & J.H. LEE. 1998. Molecular characterization of a neuronal low-voltage-activated T-type calcium channel. *Nature* **391**: 896–900.
20. CRIBBS L.L., J.H. LEE, J. YANG, J. SATIN, Y. ZHANG, A. DAUD, J. BARCLAY, M.P. WILLIAMSON, M. FOX, M. REES & E. PEREZ-REYES. 1998. Cloning and characterization of alpha1H from human heart, a member of the T-type Ca²⁺ channel gene family. *Circ. Res.* **83**: 103–109.
21. BECH-HANSEN, N.T., M.J. NAYLOR, T.A. MAYBAUM, W.G. PEARCE, B. KOOP, G.A. FISHMAN, M. METS, M.A. MUSARELLA & K.M. BOYCOTT. 1998. Loss-of-function mutations in a calcium-channel α_1 -subunit gene in Xp11.23 cause incomplete X-linked congenital stationary night blindness. *Nature Neurosci.* **19**: 264–267.
22. LACERDA, A.E., H.S. KIM, P. RUTH, E. PEREZ-REYES, V. FLOCKERZI, F. HOFMAN, L. BIRNBAUMER & A.M. BROWN. 1991. Normalization of current kinetics by interaction between the α_1 and β subunits of the skeletal muscle dihydropyridine-sensitive Ca²⁺ channel. *Nature* **352**: 527–530.
23. PEREZ-REYES, E., A. CASTELLANO, H.S. KIM, P. BERTRAND, E. BAGGSTROM, A.E. LACERDA, X. WEI & L. BIRNBAUMER. (1992). Cloning and expression of a cardiac/brain β subunit of the L-type calcium channel. *J. Biol. Chem.* **267**: 1792–1797.
24. STEPA, A., W.J. TOMLINSON, T.W. SOONG, E. BOURINET, S.J. DUBEL, S.R. VINCENT & T.P. SNUTCH. 1994. Localization and functional properties of a rat brain α_{1A} calcium channel reflect similarities to neuronal Q- and P-type channels. *Proc. Natl. Acad. Sci. USA* **91**: 10576–10580.
25. SNUTCH, T. P., W.J. TOMLINSON, J.P. LEONARD & M.M. GILBERT. 1991. Distinct calcium channels are generated by alternative splicing and are differentially expressed in the mammalian CNS. *Neuron* **7**: 45–57.
26. SOLDATOV, N.M. 1994. Genomic structure of human L-type Ca²⁺ channel. *Genomics* **22**: 77–87.
27. IHARA, Y., Y. YAMADA, Y. FUJII, T. GONOI, H. YANO, K. YASUDA, N. INAGAKI, Y. SEINO & S. SEINO. 1995. Molecular diversity and functional characterization of voltage-dependent calcium channels (CACN4) expressed in pancreatic beta-cells. *Mol. Endocrinol.* **9**: 121–130.
28. DUBEL, S.J., T.V.B. STARR, J. HELL, M.K. AHLJANIAN, J.J. ENYEART, W.A. CATTERALL, & T.P. SNUTCH. 1992. Molecular cloning of the α_1 subunit of an ω -conotoxin-sensitive calcium channel. *Proc. Natl. Acad. Sci. USA* **89**: 5058–5062.

29. STEA, A., S.J. DUBEL, M. PRAGNELL, J.P. LEONARD, K.P. CAMPBELL & T.P. SNUTCH. 1993. A β subunit normalizes the electrophysiological properties of a cloned N-type Ca channel α_1 subunit. *Neuropharmacology* **32**: 1103–1116.
30. DUBEL, S.J., A. STEA, & T.P. SNUTCH. 1994. Two cloned rat brain N-type calcium channels have distinct kinetics. *Soc. Neurosci. Abstr.* 268.12.
31. STEA, A., T.W. SOONG & T.P. SNUTCH. 1995. Determinants of PKC-dependent modulation of a family of neuronal calcium channels. *Neuron* **15**: 929–940.
32. LIN, Z., S. HAUS, J. EDGERTON & D. LIPSCOMBE. 1997. Identification of functionally distinct isoforms of the N-type Ca^{2+} channel in rat sympathetic ganglia and brain. *Neuron* **18**: 153–166.
33. WILLIAMS, M.E., P.F. BRUST, D.H. FELDMAN, S. PATTHI, S. SIMERSON, A. MAROUFI, A.F. McCUE, G. VELICELEBI, S.B. ELLIS & M. HARPOLD. 1992. Structure and functional expression of an ω -conotoxin-sensitive human N-type calcium channel. *Science* **257**: 389–395.
34. FUJITA, Y., M. MYNLIFF, R.T. DIRKSEN, M. KIM, T. NIIDOME, J. NAKAI, T. FRIEDRICH, N. IWABE, T. MIYATA, T. FURUICHI, D. FURUTAMA, K. MIKOSHIBA, Y. MORI & K.G. BEAM. 1993. Primary structure and functional expression of the ω -conotoxin-sensitive N-type calcium channel from rabbit brain. *Neuron* **10**: 585–598.
35. COPPOLA, T., R. WALDMANN, M. BORSOTTO, C. HEURTEAUX, G. ROMÉY, M.-G. MATTEI & M. LAZDUNSKI. 1994. Molecular cloning of a murine N-type calcium channel α_1 subunit. Evidence for isoforms, brain distribution and chromosomal localization. *FEBS Lett.* **338**: 1–5.
36. SWICK, A.G., M. JANICOT, T. CHENEVAL-KASTELIC, J.C. MCLLENITHAN & M.D. LANE. 1992. Promoter-cDNA-directed heterologous protein expression in *Xenopus laevis* oocytes. *Proc. Natl. Acad. Sci. USA* **89**: 1812–1816.
37. BOURINET, E., T.W. SOONG, A. STEA & T.P. SNUTCH. 1996. Determinants of the G-protein dependent opioid modulation of neuronal calcium channels. *Proc. Natl. Acad. Sci. USA* **93**: 1486–1491.
38. ZAMPONI, G.W., E. BOURINET, D. NELSON, J. NARGEOT & T.P. SNUTCH. 1997. Crosstalk between G proteins and protein kinase C mediated by the calcium channel α_1 subunit. *Nature* **385**: 242–246.
39. TANABE, T., K.G. BEAM, B.A. ADAMS, T. NIIDOME & S. NUMA. 1990. Regions of the skeletal muscle dihydropyridine receptor critical for excitation-contraction coupling. *Nature* **346**: 567–569.
40. YANG, J. P.T. ELLINOR, W.A. SATHER, J.-F. ZHANG & R.W. TSIEN. 1993. Molecular determinants of Ca^{2+} selectivity and ion permeation in L-type Ca^{2+} channels. *Nature* **366**: 158–161.
41. NAKAI, J., B.A. ADAMS, K. IMOTO & K.G. BEAM. 1994. Critical roles of the S3-S4 linker of repeat I in activation of L-type calcium channels. *Proc. Natl. Acad. Sci. USA* **91**: 1014–1018.
42. PRAGNELL, M., M. DE WAARD, Y. MORI, T. TANABE, T.P. SNUTCH & K.P. CAMPBELL. 1994. Calcium channel β subunit binds to a conserved motif in the I-II cytoplasmic linker of the α_1 subunit. *Nature* **368**: 68–70.